ISSN: 2689-1204

Research Article

Journal of Applied Material Science & Engineering Research

Analysis of Coupled Dynamic and Voltage Models of Piezoelectric Cantilever Energy Harvester using Differential Transformation Method

M G Sobamowo, AN Okorie and MO Oyekeye

Department of Mechanical Engineering, University of Lagos, Nigeria

***Corresponding author**
M G Sobamowo, Department of Mechanical Engineering, University of Lagos, Nigeria

Submitted: 08 July 2020; **Accepted**: 15 July 2020; **Published**: 07 Sep 2020

Abstract

In this work, differential transformation method with after treatment technique is applied to develop analytical models for the prediction of the behavior and output voltage of cantilever piezoelectric energy harvesters. The analytical results are in a good agreement with the experimental results in literature. The first mode of vibration has the lowest resonant frequency, and typically provides the most deflection and therefore electrical energy. The output voltage increases with the length of the beam but increase in the thickness of the beam decreases the output voltage. The results depict that the shape of the cantilever energy harvester plays an important role in improving the harvester's efficiency. It is established that under the same loading, material and geometrical conditions, triangular cantilever beams are more efficient than rectangular ones. From the results, it is also established that that among all the cantilever beams with uniform thickness, the triangular cantilever, can lead to highest resonance frequency. Therefore, in order to obtain more wideband piezoelectric energy harvester, the geometrical and material designs of piezoelectric resonant cantilevers must be properly analyzed.

Keywords: Energy Harvesters; Cantilever Beam; Piezoelectric; Output Voltage; Differential Transformation Method

Introduction

Indisputably, well established technologies have been designed and employed for macro-scale and high powered machines and technologies. However, the lack of cables induces a constraint on power supply for low powered wireless electronic sensors. Also, batteries wear out with time, therefore, regular replacement is an integral and inevitable part of maintenance for low powered electronics devices. Employing dense network in the structures, batteries replacement becomes a major time-consuming task that is uneconomical and unmanageable. Harvesting energy from ambient vibrations, wind, heat or light could enable smart sensors to be functional indefinitely [1].

Energy harvesting of scavenging is the conversion of ambient energy in the environment surroundings into electrical energy. Energy harvesters have been designed to capture the ambient energy and to convert it to usable electrical power for supplying micro scale energy harvesting technologies, low powered electronics devices and sensors. The goal is to develop autonomous and self-powered devices that do not need any replacement of traditional electrochemical batteries. In the class of energy harvesters, there is Vibration energy harvesting device called piezoelectric which converts the kinetic energy from vibration into electrical energy. The vibration can come from any source such seismic (ground) vibrations, acoustic pressure waves, forces applied directly to the load on the working surface or other surrounding sources. Vibration energy harvesting can be achieved by using electrostatic devices, electromagnetic field and utilizing piezoelectric based materials [1-2]. However, vibration energy harvesting with the piezoelectric material can currently generate up to 300 microwatts per cubic centimeter, making it an attractive method of powering low-power electronics. Consequently, different studies have carried to analyze and investigation the energy harvesting capabilities of piezoelectric devices. In a recent work, Hosseini and Hamedi explored the geometry of piezoelectric bimorphs to enhance the capabilities of energy harvesting [3]. The same authors presented another study on the resonant frequency of unimorph triangular V-shaped piezoelectric cantilever energy harvester [4]. Baker et al. also explored the geometries of the structure to increase the power density of the energy harvesters [5]. Anderson and Sexton presented sensor platform for vibration energy harvesting [6]. Beeby et al. submitted on a study on energy harvesting for microsystems applications [7]. Erturk and Inman developed a distributed parameter electromechanical model for cantilevered piezoelectric energy harvesters. Effects of length/width ratio of tapered beams on the performance

of piezoelectric energy harvesters were investigated by Matova et al. [9]. More studies on effects of geometry, optimization, design, sensitivity analysis and parameters identifications by other authors [10-27].

It is well established form the review studies that the geometry of a piezoelectric cantilever beam will greatly affect its vibration energy harvesting ability. However, the need for symbolic and precise analytical models for predicting the dynamic behavior and the corresponding output voltage for the difference geometries of the piezoelectric cantilevers cannot be overemphasized. Therefore, in this work, differential transformation method with after treatment technique is applied to develop analytical models for the prediction of the dynamic behavior and output voltage of cantilever piezoelectric energy harvesters. Parametric studies are carried out and the results are presented.

Model Formulation

Consider a structure of unimorph piezoelectric rectangular cantilever is shown in Fig. 1. In Fig. 1, Because of the low thickness of the beam, Euler-Bernoulli theory is considered in deriving the mathematical modeling of the structure.

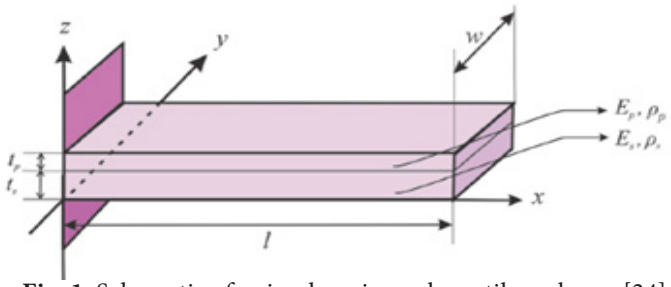

Fig. 1. Schematic of a simple unimorph cantilever beam [24]

The governing equation of motion for a beam embedded by a single piezoelectric layer under the influence of base excitation is as follows [16, 27]:

$$\frac{\partial^2}{\partial x^2}\left(EI(x)\frac{\partial^2 z_{rel}}{\partial x^2}\right)+\frac{\partial^2}{\partial x^2}\left(C_z I(x)\frac{\partial^3 z_{rel}}{\partial x^2 \partial t}\right)+m(x)\frac{\partial^2 z_{rel}}{\partial t^2}+C_a\frac{\partial z_{rel}}{\partial t}$$
$$+\frac{\partial^2}{\partial x^2}\left(\eta(x)v(t)\left[\frac{d\delta(x)}{dx}-\frac{d\delta(x-l)}{dx}\right)\right)=-(m(x)+M_t\delta(x-l))\frac{\partial^2 z_b}{\partial t^2} \quad (1)$$

If we assumed constant mass and second moment of inertia, we have

$$EI\frac{\partial^4 z_{rel}}{\partial x^4}+C_z I\frac{\partial^5 z_{rel}}{\partial x^4 \partial t}+m\frac{\partial^2 z_{rel}}{\partial t^2}+C_a\frac{\partial z_{rel}}{\partial t}$$
$$+\eta v(t)\left(\left[\frac{d^3\delta(x)}{dx^3}-\frac{d^3\delta(x-l)}{dx^3}\right)\right)=-(m+M_t\delta(x-l))\frac{\partial^2 z_b}{\partial t^2} \quad (2)$$

Subjected to the following initial and the boundary conditions

Initial conditions

$$z(x,0)=z_o,\quad \frac{\partial z(x,0)}{\partial t}=u_0, \quad (3)$$

Boundary conditions

$$z(0,t)=0,\quad \frac{\partial z(0,t)}{\partial x}=0,\quad EI\frac{\partial^2 z(L,t)}{\partial x^2}=0,\quad \frac{\partial^3 z(L,t)}{\partial x^3}=0, \quad (4)$$

The voltage equation is given as (Hosseini et al., 2019)

$$\frac{\partial v}{\partial t}+\frac{t_p}{\varepsilon_{33}^z w(x) l R_L}v==\frac{d_{31}\left(\frac{t_s}{2}+t_p\right)E_p t_p}{\varepsilon_{33}^z l}\int_{x=0}^{x=l}\frac{\partial^3 z_{rel}}{\partial x^2 \partial t}dx \quad (5)$$

Initial conditions

$$V(0)=V_0 \quad (6)$$

In this work, the base excitation, *zb* is given as

$$Z_b(x,t)=ZoW_b(X)sin\omega t \quad (7)$$

Method of Solution using Differential Transform Method

The relatively new approximate analytical method, differential transformation method is used to analyze the phenomena under investigation. The differential transformation method (DTM) has proven to be more effective than most of the other approximate analytical methods as it does not require many computations. It solves nonlinear problems without linearization, discretization, restrictive assumptions, perturbation and discretization or round-off error. It is capable of greatly reducing the size of computational work while still accurately providing the series solution with fast convergence rate. Also, it reduces the complexity of expansion of derivatives and the computational difficulties of the other traditional and approximation analytical methods [28]. The advantage of using DTM is the possibility for dealing with wide range of excitation frequency. Using the approximate method, the effects of the nonlinear parameters in the model equation on the dynamic response of the beam are investigated.

Using the Galerkin's decomposition procedure to separate the spatial and temporal parts of the transverse displacement functions,

$$z_{rel}(x,t)=\sum_{k=1}^{\infty}w_k(x)q_k(t) \quad (8)$$

where $z_{rel}(x,t)$ is the transverse displacement functions, $_{qk}(t)$ is generalized coordinate of the system is the time-dependent parameter of the oscillation, N is number of assume modes and $w_k(x)$ is the k-mode shape of the cantilever beam or a trial/comparison function that will satisfy both the geometric and natural boundary conditions. The trial function is given as

$$w_k(x)=(\cos(\beta_k x)-\cosh(\beta_k x))-\left(\frac{\cos(\beta_k l)+\cosh(\beta_k l)}{\sin(\beta_k l)+\sinh(\beta_k l)}\right)(\sin(\beta_k x)-\sinh(\beta_k x)) \quad (9)$$

For the four first-modes of linear cantilever beam, the parameters *β1* are given in Table 1.

Table 1: The four first-modes of linear cantilever beam

i	$\beta_k l$	$\omega_k (rad/s)$
1	1.8751	15.6762
2	4.6941	98.2410
3	7.8548	275.0800
4	10.9955	539.0360

The natural frequencies for the four mode shapes are shown in Table 1. It is shown in the Table that the margins between the frequencies are quite large.

Substitute Eq. (8) and Eq. (9) for the first mode shape of the cantilever beam into Eq. (2) and (5) and apply the Galerkin decomposition method. After collecting the like terms, the following equation is obtained:

$$\frac{d^2q(t)}{dt^2}+2\zeta\omega_k\frac{dq(t)}{dt}+\omega_k^2q(t)+\eta\frac{dw_k(x)}{dx}\bigg|_{x=l}v(t)=\left[\int_0^l w_k(x)m(x)dx+Mw_k(l)\right]\frac{d^2w_b(x)}{dx^2} \quad (10)$$

$$\frac{\partial v(t)}{\partial t}+\frac{t_p}{\varepsilon_{33}^s w(x)lR_L}v(t)=-\sum_{k=1}^{\infty}\frac{d_{31}E_p h_p\left(\frac{h_s}{2}+h_p\right)}{\varepsilon_{33}^s L}\frac{d^2w_k(x)}{dx^2}\bigg|_{x=L}\frac{dq_k(t)}{dt} \quad (11)$$

Determination of Displacement-Voltage Equation of the Beam

In this section, the application of differential equation for the transverse displacement of the beam is presented. The dynamic and voltage equations in Eqs. (10) and (11) are solved using the differential transformation method.

Method of Solution using Differential Transform Method

The basic definitions and the operational properties of the differential transformation method are given in our previous work [27]. Applications of differential transform method to the nonlinear Eqs. (10) and (11) give the DTM recursive relations as

$$(i+1)(i+2)Q_{i+2}+2\zeta\omega_k(i+1)Q_{i+1}+\omega_k^2Q_i+\eta\frac{dw_k(x)}{dx}\bigg|_{x=l}V_i=\left[\int_0^l w_k(x)m(x)dx+Mw_k(l)\right](i+1)(i+2)w_{b(i+2)} \quad (12)$$

$$(i+1)V_{i+1}+\frac{t_p}{\varepsilon_{33}^s wlR_L}V_i=-\sum_{k=1}^{\infty}\frac{d_{31}E_p h_p\left(\frac{h_s}{2}+h_p\right)}{\varepsilon_{33}^s L}\frac{d^2w_k(x)}{dx^2}\bigg|_{x=L}(i+1)Q_{i+1} \quad (13)$$

After re-arrangement of Eqs. (12) and (13), we have

$$Q_{i+2}=\frac{1}{(i+1)(i+2)}\left\{\left[\int_0^l w_k(x)m(x)dx+Mw_k(l)\right](i+1)(i+2)w_{b(i+2)}-2\zeta\omega_k(i+1)Q_{i+1}-\omega_k^2Q_i-\eta\frac{dw_k(x)}{dx}\bigg|_{x=l}V_i\right\} \quad (14)$$

$$V_{i+1}=\frac{-1}{(i+1)}\left\{\sum_{k=1}^{\infty}\frac{d_{31}E_p h_p\left(\frac{h_s}{2}+h_p\right)}{\varepsilon_{33}^s L}\frac{d^2w_k(x)}{dx^2}\bigg|_{x=L}(i+1)Q_{i+1}+\frac{t_p}{\varepsilon_{33}^s wlR_L}V_i\right\} \quad (15)$$

And the transformed initial conditions expressed as;

$$Q_0=z_0,\ Q_0=u_0,\ V_0=v_0, \quad (16)$$

Using the transformed conditions on the transformed governing equation, the term by term solution becomes;

$$Q_2=\frac{1}{2}\left\{2\left[\int_0^l w_k(x)m(x)dx+Mw_k(l)\right]w_{b,2}-2\zeta\omega_kQ_1-\omega_k^2Q_0-\eta\frac{dw_k(x)}{dx}\bigg|_{x=l}V_0\right\}$$

$$Q_3=\frac{1}{6}\left\{6\left[\int_0^l w_k(x)m(x)dx+Mw_k(l)\right]w_{b,3}-4\zeta\omega_kQ_2-\omega_k^2Q_1-\eta\frac{dw_k(x)}{dx}\bigg|_{x=l}V_1\right\}$$

$$Q_4=\frac{1}{12}\left\{12\left[\int_0^l w_k(x)m(x)dx+Mw_k(l)\right]w_{b,4}-6\zeta\omega_kQ_3-\omega_k^2Q_2-\eta\frac{dw_k(x)}{dx}\bigg|_{x=l}V_2\right\}$$

$$Q_5=\frac{1}{20}\left\{20\left[\int_0^l w_k(x)m(x)dx+Mw_k(l)\right]w_{b,5}-8\zeta\omega_kQ_4-\omega_k^2Q_3-\eta\frac{dw_k(x)}{dx}\bigg|_{x=l}V_3\right\}$$

$$Q_6=\frac{1}{30}\left\{30\left[\int_0^l w_k(x)m(x)dx+Mw_k(l)\right]w_{b,6}-10\zeta\omega_kQ_5-\omega_k^2Q_4-\eta\frac{dw_k(x)}{dx}\bigg|_{x=l}V_4\right\}$$

$$Q_7=\frac{1}{42}\left\{42\left[\int_0^l w_k(x)m(x)dx+Mw_k(l)\right]w_{b,7}-12\zeta\omega_kQ_6-\omega_k^2Q_5-\eta\frac{dw_k(x)}{dx}\bigg|_{x=l}V_5\right\}$$

$$Q_8=\frac{1}{56}\left\{56\left[\int_0^l w_k(x)m(x)dx+Mw_k(l)\right]w_{b,8}-14\zeta\omega_kQ_7-\omega_k^2Q_6-\eta\frac{dw_k(x)}{dx}\bigg|_{x=l}V_6\right\}$$

$$Q_9=\frac{1}{72}\left\{72\left[\int_0^l w_k(x)m(x)dx+Mw_k(l)\right]w_{b,9}-16\zeta\omega_kQ_8-\omega_k^2Q_7-\eta\frac{dw_k(x)}{dx}\bigg|_{x=l}V_7\right\}$$

$$Q_{10}=\frac{1}{90}\left\{90\left[\int_0^l w_k(x)m(x)dx+Mw_k(l)\right]w_{b,10}-18\zeta\omega_kQ_9-\omega_k^2Q_8-\eta\frac{dw_k(x)}{dx}\bigg|_{x=l}V_8\right\}$$

$$Q_{11}=\frac{1}{110}\left\{110\left[\int_0^l w_k(x)m(x)dx+Mw_k(l)\right]w_{b,11}-20\zeta\omega_kQ_{10}-\omega_k^2Q_9-\eta\frac{dw_k(x)}{dx}\bigg|_{x=l}V_8\right\}$$

$$V_1=-\left\{\sum_{k=1}^{\infty}\frac{d_{31}E_p h_p\left(\frac{h_s}{2}+h_p\right)}{\varepsilon_{33}^s L}\frac{d^2w_k(x)}{dx^2}\bigg|_{x=L}Q_1+\frac{t_p}{\varepsilon_{33}^s w(x)lR_L}V_0\right\}$$

$$V_2=\frac{-1}{2}\left\{2\sum_{k=1}^{\infty}\frac{d_{31}E_p h_p\left(\frac{h_s}{2}+h_p\right)}{\varepsilon_{33}^s L}\frac{d^2w_k(x)}{dx^2}\bigg|_{x=L}Q_2+\frac{t_p}{\varepsilon_{33}^s w(x)lR_L}V_1\right\}$$

$$V_3=\frac{-1}{3}\left\{3\sum_{k=1}^{\infty}\frac{d_{31}E_p h_p\left(\frac{h_s}{2}+h_p\right)}{\varepsilon_{33}^s L}\frac{d^2w_k(x)}{dx^2}\bigg|_{x=L}Q_3+\frac{t_p}{\varepsilon_{33}^s wlR_L}V_2\right\}$$

$$V_4=\frac{-1}{4}\left\{4\sum_{k=1}^{\infty}\frac{d_{31}E_p h_p\left(\frac{h_s}{2}+h_p\right)}{\varepsilon_{33}^s L}\frac{d^2w_k(x)}{dx^2}\bigg|_{x=L}Q_{i+1}+\frac{t_p}{\varepsilon_{33}^s wlR_L}V_3\right\}$$

$$V_5 = \frac{-1}{5}\left\{5\sum_{k=1}^{\infty}\frac{d_{31}E_p h_p\left(\frac{h_s}{2}+h_p\right)}{\varepsilon_{33}^s L}\frac{d^2w_k(x)}{dx^2}\bigg|_{x=L} Q_5 + \frac{t_p}{\varepsilon_{33}^s wlR_L}V_4\right\}$$

$$V_6 = \frac{-1}{6}\left\{6\sum_{k=1}^{\infty}\frac{d_{31}E_p h_p\left(\frac{h_s}{2}+h_p\right)}{\varepsilon_{33}^s L}\frac{d^2w_k(x)}{dx^2}\bigg|_{x=L} Q_{i+1} + \frac{t_p}{\varepsilon_{33}^s wlR_L}V_5\right\}$$

$$V_7 = \frac{-1}{7}\left\{7\sum_{k=1}^{\infty}\frac{d_{31}E_p h_p\left(\frac{h_s}{2}+h_p\right)}{\varepsilon_{33}^s L}\frac{d^2w_k(x)}{dx^2}\bigg|_{x=L} Q_7 + \frac{t_p}{\varepsilon_{33}^s wlR_L}V_6\right\}$$

$$V_8 = \frac{-1}{8}\left\{8\sum_{k=1}^{\infty}\frac{d_{31}E_p h_p\left(\frac{h_s}{2}+h_p\right)}{\varepsilon_{33}^s L}\frac{d^2w_k(x)}{dx^2}\bigg|_{x=L} Q_8 + \frac{t_p}{\varepsilon_{33}^s wlR_L}V_7\right\}$$

$$V_9 = \frac{-1}{9}\left\{9\sum_{k=1}^{\infty}\frac{d_{31}E_p h_p\left(\frac{h_s}{2}+h_p\right)}{\varepsilon_{33}^s L}\frac{d^2w_k(x)}{dx^2}\bigg|_{x=L} Q_9 + \frac{t_p}{\varepsilon_{33}^s wlR_L}V_8\right\}$$

$$V_{10} = \frac{-1}{10}\left\{10\sum_{k=1}^{\infty}\frac{d_{31}E_p h_p\left(\frac{h_s}{2}+h_p\right)}{\varepsilon_{33}^s L}\frac{d^2w_k(x)}{dx^2}\bigg|_{x=L} Q_{10} + \frac{t_p}{\varepsilon_{33}^s wlR_L}V_9\right\}$$

$$V_{11} = \frac{-1}{11}\left\{11\sum_{k=1}^{\infty}\frac{d_{31}E_p h_p\left(\frac{h_s}{2}+h_p\right)}{\varepsilon_{33}^s L}\frac{d^2w_k(x)}{dx^2}\bigg|_{x=L} Q_{11} + \frac{t_p}{\varepsilon_{33}^s wlR_L}V_{10}\right\}$$

After substitution of the initial conditions

$$Q_2 = \frac{1}{2}\left\{3\left[\int_0^l w_k(x)m(x)dx + Mw_k(l)\right]w_b(3) - 2\zeta\omega_k u_0 - \omega_k^2 z_0 - \eta\frac{dw_k(x)}{dx}\bigg|_{x=i} v_0\right\}$$

$$V_1 = -\left\{\sum_{k=1}^{\infty}\frac{d_{31}E_p h_p\left(\frac{h_s}{2}+h_p\right)}{\varepsilon_{33}^s L}\frac{d^2w_k(x)}{dx^2}\bigg|_{x=L} u_0 + \frac{t_p}{\varepsilon_{33}^s w(x)lR_L}v_0\right\}$$

$$Q_3 = \frac{1}{6}\left\{\begin{array}{l}\left[\int_0^l w_k(x)m(x)+Mw_k(l)\right]\frac{d^2w_b(x)}{dx^2} \\ -4\zeta\omega_k\frac{1}{2}\left\{\left[\int_0^l w_k(x)m(x)+Mw_k(l)\right]\frac{d^2w_b(x)}{dx^2} - 2\zeta\omega_k u_0 - \omega_k^2 z_0 - \eta\frac{dw_k(x)}{dx}\bigg|_{x=i} v_0\right\} \\ +\omega_k^2 u_0 - \eta\frac{dw_k(x)}{dx}\bigg|_{x=i}\left\{\sum_{k=1}^{\infty}\frac{d_{31}E_p h_p\left(\frac{h_s}{2}+h_p\right)}{\varepsilon_{33}^s L}\frac{d^2w_k(x)}{dx^2}\bigg|_{x=L} u_0 + \frac{t_p}{\varepsilon_{33}^s w(x)lR_L}v_0\right\}\end{array}\right\}$$

$$V_2 = \frac{-1}{2}\left\{\begin{array}{l}\left\{\sum_{k=1}^{\infty}\frac{d_{31}E_p h_p\left(\frac{h_s}{2}+h_p\right)}{\varepsilon_{33}^s L}\frac{d^2w_k(x)}{dx^2}\bigg|_{x=L}\left\{\begin{array}{l}\left[\int_0^l w_k(x)m(x)+Mw_k(l)\right]\frac{d^2w_b(x)}{dx^2} \\ -2\zeta\omega_k u_0 - \omega_k^2 z_0 - \eta\frac{dw_k(x)}{dx}\bigg|_{x=i} v_0\end{array}\right\}\right\} \\ -\frac{t_p}{\varepsilon_{33}^s w(x)lR_L}\left\{\sum_{k=1}^{\infty}\frac{d_{31}E_p h_p\left(\frac{h_s}{2}+h_p\right)}{\varepsilon_{33}^s L}\frac{d^2w_k(x)}{dx^2}\bigg|_{x=L} u_0 + \frac{t_p}{\varepsilon_{33}^s w(x)lR_L}v_0\right\}\end{array}\right\}$$

$$Q_4 = \frac{1}{12}\left\{\left[\int_0^l w_k(x)m(x)+Mw_k(l)\right]\frac{d^2w_b(x)}{dx^2} - 6\zeta\omega_k Q_3 - \omega_k^2 Q_2 - \eta\frac{dw_k(x)}{dx}\bigg|_{x=i} V_2\right\}$$

$$V_3 = \frac{-1}{3}\left\{3\sum_{k=1}^{\infty}\frac{d_{31}E_p h_p\left(\frac{h_s}{2}+h_p\right)}{\varepsilon_{33}^s L}\frac{d^2w_k(x)}{dx^2}\bigg|_{x=L} Q_3 + \frac{t_p}{\varepsilon_{33}^s wlR_L}V_2\right\}$$

$$Q_5 = \frac{1}{20}\left\{\left[\int_0^l w_k(x)m(x)+Mw_k(l)\right]\frac{d^2w_b(x)}{dx^2} - 8\zeta\omega_k Q_4 - \omega_k^2 Q_3 - \eta\frac{dw_k(x)}{dx}\bigg|_{x=i} V_3\right\}$$

$$V_4 = \frac{-1}{4}\left\{4\sum_{k=1}^{\infty}\frac{d_{31}E_p h_p\left(\frac{h_s}{2}+h_p\right)}{\varepsilon_{33}^s L}\frac{d^2w_k(x)}{dx^2}\bigg|_{x=L} Q_{i+1} + \frac{t_p}{\varepsilon_{33}^s wlR_L}V_3\right\}$$

$$Q_6 = \frac{1}{30}\left\{\left[\int_0^l w_k(x)m(x)+Mw_k(l)\right]\frac{d^2w_b(x)}{dx^2} - 10\zeta\omega_k Q_5 - \omega_k^2 Q_4 - \eta\frac{dw_k(x)}{dx}\bigg|_{x=i} V_4\right\}$$

$$V_5 = \frac{-1}{5}\left\{5\sum_{k=1}^{\infty}\frac{d_{31}E_p h_p\left(\frac{h_s}{2}+h_p\right)}{\varepsilon_{33}^s L}\frac{d^2w_k(x)}{dx^2}\bigg|_{x=L} Q_5 + \frac{t_p}{\varepsilon_{33}^s wlR_L}V_4\right\}$$

$$Q_7 = \frac{1}{42}\left\{\left[\int_0^l w_k(x)m(x)+Mw_k(l)\right]\frac{d^2w_b(x)}{dx^2} - 12\zeta\omega_k Q_6 - \omega_k^2 Q_5 - \eta\frac{dw_k(x)}{dx}\bigg|_{x=i} V_5\right\}$$

$$V_6 = \frac{-1}{6}\left\{6\sum_{k=1}^{\infty}\frac{d_{31}E_p h_p\left(\frac{h_s}{2}+h_p\right)}{\varepsilon_{33}^s L}\frac{d^2w_k(x)}{dx^2}\bigg|_{x=L} Q_{i+1} + \frac{t_p}{\varepsilon_{33}^s wlR_L}V_5\right\}$$

$$Q_8 = \frac{1}{56}\left\{\left[\int_0^l w_k(x)m(x)+Mw_k(l)\right]\frac{d^2w_b(x)}{dx^2} - 14\zeta\omega_k Q_7 - \omega_k^2 Q_6 - \eta\frac{dw_k(x)}{dx}\bigg|_{x=i} V_6\right\}$$

$$V_7 = \frac{-1}{7}\left\{7\sum_{k=1}^{\infty}\frac{d_{31}E_p h_p\left(\frac{h_s}{2}+h_p\right)}{\varepsilon_{33}^s L}\frac{d^2w_k(x)}{dx^2}\bigg|_{x=L} Q_7 + \frac{t_p}{\varepsilon_{33}^s wlR_L}V_6\right\}$$

$$Q_9 = \frac{1}{72}\left\{\left[\int_0^l w_k(x)m(x)+Mw_k(l)\right]\frac{d^2w_b(x)}{dx^2} - 16\zeta\omega_k Q_8 - \omega_k^2 Q_7 - \eta\frac{dw_k(x)}{dx}\bigg|_{x=i} V_7\right\}$$

$$V_8 = \frac{-1}{8}\left\{8\sum_{k=1}^{\infty}\frac{d_{31}E_p h_p\left(\frac{h_s}{2}+h_p\right)}{\varepsilon_{33}^s L}\frac{d^2w_k(x)}{dx^2}\bigg|_{x=L} Q_8 + \frac{t_p}{\varepsilon_{33}^s wlR_L}V_7\right\}$$

$$Q_{10} = \frac{1}{90}\left\{\left[\int_0^l w_k(x)m(x)+Mw_k(l)\right]\frac{d^2w_b(x)}{dx^2} - 18\zeta\omega_k Q_9 - \omega_k^2 Q_8 - \eta\frac{dw_k(x)}{dx}\bigg|_{x=i} V_8\right\}$$

$$V_9 = \frac{-1}{9}\left\{9\sum_{k=1}^{\infty}\frac{d_{31}E_p h_p\left(\frac{h_s}{2}+h_p\right)}{\varepsilon_{33}^s L}\frac{d^2w_k(x)}{dx^2}\bigg|_{x=L} Q_9 + \frac{t_p}{\varepsilon_{33}^s wlR_L}V_8\right\}$$

$$Q_{11} = \frac{1}{110}\left\{\left[\int_0^l w_k(x)m(x)+Mw_k(l)\right]\frac{d^2w_b(x)}{dx^2} - 20\zeta\omega_k Q_{10} - \omega_k^2 Q_9 - \eta\frac{dw_k(x)}{dx}\bigg|_{x=i} V_9\right\}$$

From the definition of the differential transform method, we have

$$Q(t)=Q_0+Q_1t+Q_2t^2+Q_3t^3+Q_4t^4+Q_5t^5+Q_6t^6+Q_7T^7+Q_8t^8+Q_9t^9+Q_{10}t^{10}+Q_{11}t^{11} \quad (17)$$

and

$$V(t)=V_0+V_1t+V_2t^2+V_3t^3+V_4t^4+V_5t^5+V_6t^6+V_7t^7+V_8t^8+V_9t^9+V_{10}t^{10}+V_{11}t^{11} \quad (18)$$

The power series solution gives solution in the form of truncated series. This truncated series is periodic only in a very small region. In order to make the solution periodic over a large range, sine and cosine-after treatment (SAT and CAT-technique).

Table2: The Beam geometry and shape function

Geometry	Visual	Shape function	Resonant Frequency
Generic	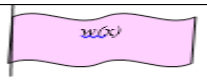	$w(x)$	$f(w(x))=\frac{\sqrt{3}}{\pi}\sqrt{\frac{E_s(t_s-h)^3+E_sh^3+E_s(t_s+t_p-h)^3+E_p(t_s-h)^3}{\rho_s t_s+\rho_p t_p}}\sqrt{\frac{\int_0^l w(x)(l-x)^2dx}{\int_0^l w(x)x^2(3l-x)^2dx}}$
Rectangular	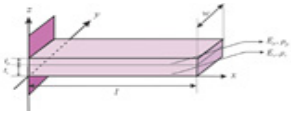	$w(x)=w$	$f_w=\frac{\sqrt{0.85}}{11\pi l_1^2}\sqrt{\frac{E_s(t_s-h)^3+E_sh^3+E_s(t_s+t_p-h)^3+E_p(t_s-h)^3}{\rho_s t_s+\rho_p t_p}}$
Triangular tapered	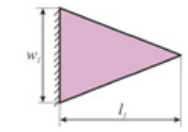	$w(x)=w_1\left(1-\frac{x}{l_1}\right)$	$f(w(x))=\frac{\sqrt{3}}{\pi}\sqrt{\frac{E_s(t_s-h)^3+E_sh^3+E_s(t_s+t_p-h)^3+E_p(t_s-h)^3}{\rho_s t_s+\rho_p t_p}}\sqrt{\frac{\int_0^l w(x)(l-x)^2dx}{\int_0^l w(x)x^2(3l-x)^2dx}}$
Trapezoidal V-shaped (Quadrilateral)	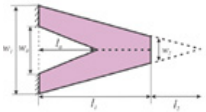	$w(x)=\begin{cases}\frac{w_1}{2}\left(1-\frac{x}{l_1+l_2}\right)-\frac{w_2}{2}\left(1-\frac{x}{l_2}\right), & x\in[0,l_2]\\ \frac{w_1}{2}\left(1-\frac{x}{l_1+l_2}\right), & x\in[l_2,l_1]\end{cases}$	$f(w(x))=\frac{\sqrt{3}}{\pi}\sqrt{\frac{E_s(t_s-h)^3+E_sh^3+E_s(t_s+t_p-h)^3+E_p(t_s-h)^3}{\rho_s t_s+\rho_p t_p}}\sqrt{\frac{\int_0^l w(x)(l-x)^2dx}{\int_0^l w(x)x^2(3l-x)^2dx}}$

Results and Discussion

Using MATLAB for the simulations, the analytical models are simulated and parametric studies are carried out. As it was well established, it should therefore be pointed out that compared to other structural forms of beams, a cantilever beam can obtain the maximum deformation and strain under the same conditions [24]. The larger deflection leads to more stress, strain, and consequently a higher output voltage and power. Therefore, the vast majority of piezoelectric vibration energy harvesting devices use a cantilever beam structure. This give reasons for the present analysis on cantilever beam as the results are presented.

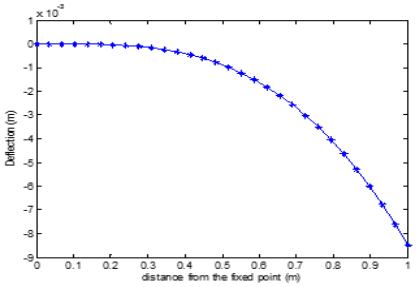

Fig. 4.1 first normalized mode shapes of the cantilever energy harvester

The sensitivity of resonant cantilever piezoelectric energy harvesters is directly proportional to the resonant frequency. It is noteworthy that a cantilever beam can have many different modes of vibration with a different resonant frequency. The first mode of vibration (Fig. 4.1) has the lowest resonant frequency, and typically provides the most deflection and therefore electrical energy. Accordingly, energy harvesters are generally designed to operate in the first resonant mode. So, the present analysis and the simulations are based on the resonant of the first resonant mode as shown in Fig. 4.1. The undamped dynamic response of the beam is presented in Fig. 4.1. The first normalized mode shapes of the beams for the cantilever beam are shown in Fig. 1 Also, the figure shows the deflection of the beams along the beams' span at buckled and mode shape. As expected, the result show that the amplitude of the vibration is maintained throughout the vibration period of the cantilever beam. However, if the damping parameter is considered, the deflection of the beam reduces as the time progresses as the energy generated by the beam reduces correspondingly.

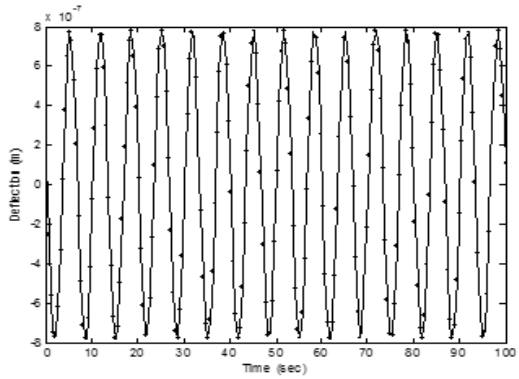

Fig. 4.2 Dynamic behavior of the cantilever energy harvester

Fig. 4.3 and 4.4 present the impacts of cantilever geometrical structure on the output voltage, from the figures, it was established that the rectangular beam produces lowest output voltage. However, a triangular tapered cantilever gives the maximum output voltage. Also, the results depict that changing the shape of the cantilevers could affect the generated output power and voltage. Therefore, in order to obtain more wideband piezoelectric energy harvester, the design of piezoelectric resonant cantilevers must be properly carried out.

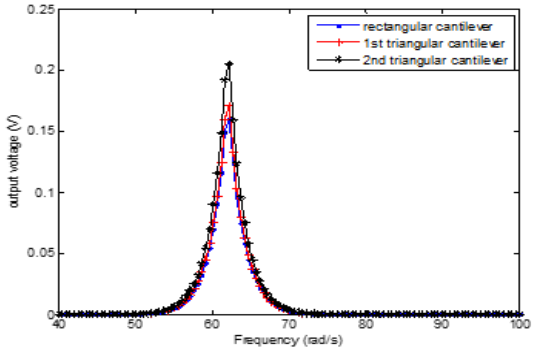

Fig. 4.3. Comparison of the results for different geometry of cantilever energy harvester

Additionally, as shown in the results, the cantilever geometrical structure plays an important role in improving the harvester's efficiency as it greatly affects its vibration energy harvesting ability. Therefore, a triangular tapered cantilever has been found to be the optimum design, because it ensures a large constant strain in the piezoelectric layer resulting in higher power output compared with the rectangular beam with the width and length equal to the base and height of the corresponding triangular tapered cantilever beam [24].

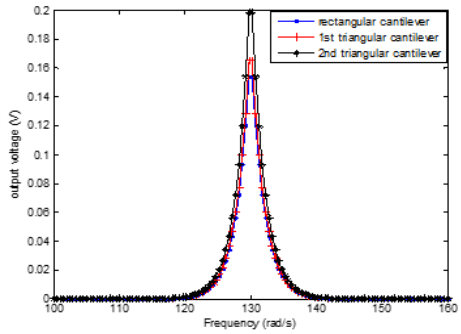

Fig. 4.4. Comparison of the experimental and analytical results for the 1st triangular cantilever energy harvester

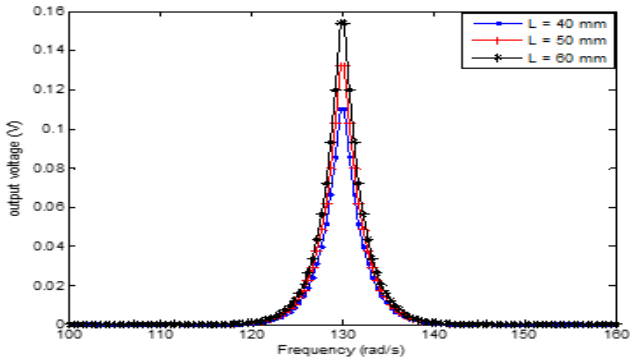

Fig. 4.5. Effect of the cantilever energy harvester length on the output voltage

Fig. 4.5 and 4.6 shows the effects of beam length and thickness on the output voltage. Although, the output voltage increases with the length of the beam, it was shown that increase in the thickness of the beam decreases the output voltage. This is because, as the thickness of the beam increases, the weight of the beam increases and deflection of the vibration decreases which consequently affect the output voltage.

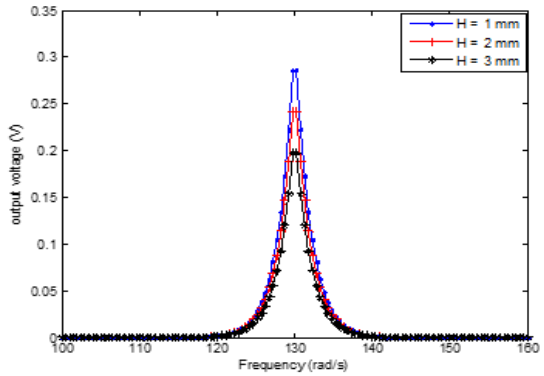

Fig. 4.6. Effect of the cantilever energy harvester thickness on the output voltage

Conclusion

In this work, differential transformation method has been used to develop a highly precise explicit analytical model for approximating the output voltage of cantilever energy harvesters. The analytical results are in a good agreement with the experimental results, and the relative error is negligible. It was established that the shape of the cantilever beam or the cantilever geometrical structure plays an important role in improving the harvester's efficiency. In fact, it was shown that under the same loading, material and geometrical conditions, triangular cantilever beams are more efficient than rectangular ones. It turns out that the shape can have a significant effect on the output voltage and therefore maximum output power density. From the results, it was established that that among all the cantilever beams with uniform thickness, the triangular cantilever can lead to highest resonance frequency. The output voltage increases with the length of the beam but increase in the thickness of the beam decreases the output voltage. The results in this work present a strong potential to be used in the design and optimization of triangular cantilever piezoelectric energy harvesters.

Nomenclature

C_a viscous air damping coefficient
C_s equivalent strain rate

E_p Young's modulus piezoelectric layers
E_s Young's modulus for substrate
f frequency of vibration,
H total thickness of the of the cantilever beam
I area moment of inertia
I_s total cross-sectional area moment of inertia
I_t rotary inertia of the tip mass
l length of the cantilever beam
M internal moment,
m mass per unit length of the beam
mt tip mass
t_p piezoelectric thickness
t_s substrates thickness
v output voltage
w width of the cantilever beam,
z transverse displacement of the neutral axis
z_b base excitation displacement
ρ_p piezoelectric density
ρ_s substrates density

References

1. N Elvin, A Erturk (2013) Advances in energy harvesting methods, Springer Science & Business Media.
2. S Beeby, N White (2014) Energy harvesting for autonomous systems, Artech House.
3. R Hosseini, M Hamed (2015) Improvements in energy harvesting capabilities by using different shapes of piezoelectric bimorphs. Journal of Micromechanics and Microengineering 25.
4. R Hosseini, M Hamedi (2015) Study of the resonant frequency of unimorph triangular V-shaped piezoelectric cantilever energy harvester. International Journal of Advanced Design and Manufacturing Technology 8.
5. J Baker, S Roundy, P Wright (2005) Alternative geometries for increasing power density in vibration energy scavenging for wireless sensor networks. In: Proceedings of the Third International Energy Conversion Engineering Conference.
6. TA Anderson, DW Sexton (2006) A vibration energy harvesting sensor platform for increased industrial efficiency. In: Smart structures and materials, International Society for Optics and Photonics 61741-61749.
7. SP Beeby, MJ Tudor, N White (2006) Energy harvesting vibration sources for microsystems applications. Measurement science and technology 17: 175.
8. A Erturk, DJ Inman (2008) A distributed parameter electromechanical model for cantilevered piezoelectric energy harvesters. Journal of vibration and acoustics, 130041002.
9. S Matova, M Renaud, M Jambunathan, M Goedbloed, R Van Schaijk, et al. (2013) Effect of length/width ratio of tapered beams on the performance of piezoelectric energy harvesters. Smart Materials and Structures 22: 075015.
10. N Siddiqui (2014) Understanding effects of tapering cantilevered piezoelectric bimorph for energy harvesting from vibrations, PhD thesis, Auburn University.
11. AG Muthalif, ND Nordin (2015) Optimal piezoelectric beam shape for single and broadband vibration energy harvesting: Modeling, simulation and experimental results. Mechanical Systems and Signal Processing 54: 417-426.
12. R Hosseini, M Hamedi (2016) An investigation into resonant frequency of trapezoidal V-shaped cantilever piezoelectric energy harvester. Microsystem Technologies 22: 1127-1134.
13. R Hosseini, M Hamedi (2016) An Investigation into Resonant Frequency of Triangular V-Shaped Cantilever Piezoelectric Vibration Energy Harvester. Journal of Solid Mechanics 8: 560-567.
14. K Yang, Z Li, Y Jing, D Chen, T Ye, et al. (2009) Research on the resonant frequency formula of V-shaped cantilevers. In: 2009 4th IEEE International Conference on Nano/Micro Engineered and Molecular Systems 59-62.
15. R Hosseini, M Hamedi (2016) Resonant frequency of bimorph triangular V-shaped piezoelectric cantilever energy harvester. Journal of Computational & Applied Research in Mechanical Engineering 6: 65-73.
16. A Erturk, DJ Inman (2011) Piezoelectric energy harvesting. John Wiley & Sons.
17. O Zargar, A Masoumi, AO Moghaddam (2017) Investigation and optimization for the dynamical behaviour of the vehicle structure. International Journal of Automotive and Mechanical Engineering 14: 4196-4210.
18. L Tang, Y Yang, CK Soh (2013) Broadband vibration energy harvesting techniques. In: Advances in energy harvesting methods, Springer 17-61.
19. S Shahruz (2006) Limits of performance of mechanical bandpass filters used in energy scavenging. Journal of sound and vibration 293: 449- 461.
20. Z Yang, J Yang (2009) Connected vibrating piezoelectric bimorph beams as a wide-band piezoelectric power harvester. Journal of Intelligent Material Systems and Structures 20: 569-574.
21. Chen Z, Yang Y, Deng G (2009) Analytical and Experimental Study on Vibration Energy Harvesting Behaviors of Piezoelectric Cantilevers with Different Geometries. In Sustainable Power Generation and Supply, 2009. SUPERGEN'09. International Conference on 1-6.
22. Shahruz S (2006) Design of Mechanical Band-pass Filters for Energy Scavenging. Journal of Sound and Vibration 292: 987-998.
23. Xue H, Hu Y, Wang QM (2008) Broadband Piezoelectric Energy Harvesting Devices using Multiple Bimorphs with Different Operating Frequencies. Ultrasonics, Ferroelectrics, and Frequency Control, IEEE Transactions on 55: 2104-2108.
24. R Hosseini, M Nouri (2016) Shape design optimization of unimorph piezoelectric cantilever energy harvester. Journal of Computational Applied Mechanics 47: 247-259.
25. R Hosseini, M Hamedi, A Ebrahimi Mamaghani, HC Kim, J Kim, et al. (2017) Parameter identification of partially covered piezoelectric cantilever power scavenger based on the coupled distributed parameter solution. International Journal of Smart and Nano Materials 8: 110-124.
26. R Hosseini, M Hamedi, J Im, J Kim, J Dayou, et al. (2017) Analytical and experimental investigation of partially covered piezoelectric cantilever energy harvester. International Jour-

nal of Precision Engineering and Manufacturing 18: 415-424.

27. R Hosseini, M Hamedi, H Golparvar, O Zargar (2019) Analytical and experimental investigation into increasing operating Bandwidth of Piezoelectric Energy Harvesters. AUT Journal of Mechanical Engineering 3: 113-122.

28. MG Sobamowo, AA Yinusa (2019) Insight into the Boundary Layer Flows of Free Convection and Heat Transfer of Nanofluids Over a Vertical Plate using Multi-Step Differential Transformation Method. Iranian Journal of Mechanical Engineering, 20: 1-42.